

---

**Research Articles: Systems/Circuits**

**Enhancement of the medial olivocochlear system prevents hidden hearing loss**

Luis E. Boero<sup>1,2</sup>, Valeria C. Castagna<sup>1</sup>, Mariano N. Di Guilmi<sup>2</sup>, Juan D. Goutman<sup>2</sup>, Ana Belén Elgoyhen<sup>1,2</sup> and María Eugenia Gómez-Casati<sup>1,2</sup>

<sup>1</sup>*Instituto de Farmacología, Facultad de Medicina, Universidad de Buenos Aires, 1121 Buenos Aires, Argentina.*

<sup>2</sup>*Instituto de Investigaciones en Ingeniería Genética y Biología Molecular, Dr. Héctor N. Torres, Consejo Nacional de Investigaciones Científicas y Técnicas, 1428 Buenos Aires, Argentina.*

DOI: 10.1523/JNEUROSCI.0363-18.2018

Received: 8 February 2018

Revised: 2 July 2018

Accepted: 9 July 2018

Published: 20 July 2018

---

**Author contributions:** L.E.B., M.N.D.G., J.D.G., A.B.E., and M.E.G.-C. designed research; L.E.B., V.C.C., and M.E.G.-C. performed research; L.E.B., V.C.C., and M.E.G.-C. analyzed data; M.E.G.-C. wrote the first draft of the paper; M.E.G.-C. edited the paper; M.E.G.-C. wrote the paper.

**Conflict of Interest:** The authors declare no competing financial interests.

This research was supported in part by Agencia Nacional de Promoción Científica y Técnica (Argentina) to J.D.G and M.E.G.-C, Pew Charitable Trust (USA) to M.E.G.-C, National Organization for Hearing Research (USA) to M.E.G.-C and J.D.G and NIH Grant R01 DC001508 (Paul A. Fuchs and A.B.E.).

Corresponding Author: María Eugenia Gómez-Casati, Ph.D., Instituto de Farmacología. Facultad de Medicina. Universidad de Buenos Aires. Address: Paraguay 2155. C1121ABG, Buenos Aires, Argentina. Phone: 54-11-52853350 E-mail: [mgomezcasati@fmed.uba.ar](mailto:mgomezcasati@fmed.uba.ar), [megomezcasati@gmail.com](mailto:megomezcasati@gmail.com)

**Cite as:** J. Neurosci ; 10.1523/JNEUROSCI.0363-18.2018

**Alerts:** Sign up at [www.jneurosci.org/cgi/alerts](http://www.jneurosci.org/cgi/alerts) to receive customized email alerts when the fully formatted version of this article is published.

Accepted manuscripts are peer-reviewed but have not been through the copyediting, formatting, or proofreading process.

Copyright © 2018 the authors

1 **Title Page**

2

3 **Title: Enhancement of the medial olivocochlear system prevents hidden hearing loss**

4 **Abbreviated Title:** Medial olivocochlear system and cochlear synaptopathy

5

6 **Authors:** Luis E. Boero<sup>1,2</sup>, Valeria C. Castagna<sup>1</sup>, Mariano N. Di Guilmi<sup>2</sup>, Juan D. Goutman<sup>2</sup>, Ana  
7 Belén Elgoyhen<sup>1,2</sup> and María Eugenia Gómez-Casati<sup>1,2</sup>

8

9 **Affiliations:** <sup>1</sup> Instituto de Farmacología, Facultad de Medicina, Universidad de Buenos Aires,  
10 1121 Buenos Aires, Argentina.

11 <sup>2</sup> Instituto de Investigaciones en Ingeniería Genética y Biología Molecular, Dr. Héctor N. Torres,  
12 Consejo Nacional de Investigaciones Científicas y Técnicas, 1428 Buenos Aires, Argentina.

13

14 **Corresponding Author:** María Eugenia Gómez-Casati, Ph.D.

15 Instituto de Farmacología. Facultad de Medicina. Universidad de  
16 Buenos Aires.

17 Address: Paraguay 2155. C1121ABG, Buenos Aires, Argentina.

18 Phone: 54-11-52853350

19 E-mail: [mgomezcasati@fmed.uba.ar](mailto:mgomezcasati@fmed.uba.ar), [megomezcasati@gmail.com](mailto:megomezcasati@gmail.com)

20

21 **Number of Pages:** 31

22 **Number of Figures:** 7

23 **Number of words Abstract:** 250

24 **Number of words Introduction:** 653

25 **Number of words Discussion:** 1591

26

27 **Conflict of Interest:** The authors declare no competing financial or non-financial interest.

28

29 **Acknowledgements:** This research was supported in part by Agencia Nacional de Promoción  
30 Científica y Técnica (Argentina) to J.D.G and M.E.G-C, Pew Charitable Trust (USA) to M.E.G-C,  
31 National Organization for Hearing Research (USA) to M.E.G-C and J.D.G and NIH Grant R01  
32 DC001508 (Paul A. Fuchs and A.B.E.).

33

34 **Author Contributions:** L.E.B, V.C.C, J.D.G, M.N.D-G, A.B.E and M.E.G-C designed research;  
35 L.E.B, V.C.C and M.E.G-C performed experiments; L.E.B, V.C.C and M.E.G-C analyzed data.  
36 M.E.G-C wrote the paper. All authors discussed the results, read and commented on the  
37 manuscript.  
38

39 **Abstract**

40 Cochlear synaptopathy produced by exposure to noise levels which only cause transient  
41 auditory threshold elevations is a condition that affects many people and is believed to  
42 contribute to poor speech discrimination in noisy environments. These functional deficits in  
43 hearing, without changes in sensitivity, have been called hidden hearing loss (HHL). It has been  
44 proposed that activity of the medial olivocochlear (MOC) system can ameliorate acoustic trauma  
45 effects. Here we explore the role of the MOC system in HHL by comparing the performance of  
46 two different mouse models: an  $\alpha 9$  nicotinic receptor subunit *knock-out* (*Chrna9* KO) which  
47 lacks cholinergic transmission between efferent neurons and hair cells, and a gain of function  
48 *knock-in* (*Chrna9L9'T* KI) carrying an  $\alpha 9$  point mutation that leads to enhanced cholinergic  
49 activity. Animals of either sex were exposed to sound pressure levels that in wild-type (WT)  
50 produced transient cochlear threshold shifts and a decrease in neural response amplitudes,  
51 together with the loss of ribbon synapses, indicative of cochlear synaptopathy. Moreover, a  
52 reduction in the number of efferent contacts to OHCs was observed. In *Chrna9* KO ears, noise  
53 exposure produced permanent auditory threshold elevations together with cochlear  
54 synaptopathy. In contrast, the *Chrna9L9'T* KI was completely resistant to the same acoustic  
55 exposure protocol. These results show a positive correlation between the degree of HHL  
56 prevention and the level of cholinergic activity. Notably, enhancement of the MOC feedback  
57 promoted new afferent synapse formation, suggesting that it can trigger cellular and molecular  
58 mechanisms to protect and/or repair the inner ear sensory epithelium.

59

60 **Significance Statement**

61 Noise overexposure is a major cause of a variety of perceptual disabilities, including speech-in-  
62 noise difficulties, tinnitus and hyperacusis. Here we show that exposure to noise levels that do  
63 not cause permanent threshold elevations nor hair cell death, can produce a loss of cochlear  
64 nerve synapses to inner hair cells (IHCs) as well as degeneration of MOC terminals contacting  
65 the outer hair cells (OHCs). Enhancement of the MOC reflex can prevent both types of  
66 neuropathy, highlighting the potential use of drugs that increase  $\alpha 9\alpha 10$  nicotinic cholinergic  
67 receptor activity as a pharmacotherapeutic strategy to avoid HHL.

68

69 **Introduction**

70 Noise-induced hearing loss (NIHL) is growing as one of the most prevalent types of non-  
71 congenital hearing loss. It has recently been shown that exposure to loud sounds, causing only  
72 transient cochlear threshold elevations, can produce a loss of synapses between IHCs and  
73 auditory nerve fibers (Kujawa and Liberman, 2009). This cochlear synaptopathy, also known as  
74 HHL (Schaette and McAlpine, 2011), occurs within hours post acoustic exposure and it is  
75 proposed to be a type of glutamate excitotoxicity (Liberman and Mulroy, 1982; Pujol et al., 1993;  
76 Pujol and Puel, 1999). Recent studies have demonstrated that auditory nerve fibers with high-  
77 threshold and low spontaneous rates (SR) are most vulnerable to noise damage compared to  
78 low-threshold high-SR fibers (Furman et al., 2013; Liberman and Liberman, 2015). These  
79 observations provide an explanation to the absence of auditory threshold elevations in cochlear  
80 synaptopathy models. Due to the wider dynamic range and threshold distribution, it was  
81 suggested that these low-SR fibers are critical for signal coding in noisy backgrounds  
82 (Costalupes, 1985; Young and Barta, 1986).

83

84 MOC efferent neurons form a negative feedback gain-control system that inhibits amplification  
85 of sounds by OHCs (Galambos, 1955; Wiederhold and Kiang, 1970; Guinan, 2011). Activation  
86 of the MOC pathway reduces cochlear sensitivity through the action of acetylcholine on  $\alpha 9\alpha 10$   
87 cholinergic nicotinic receptors (nAChRs) at the base of OHCs (Elgoyhen et al., 1994, 2001;  
88 Ballesterro et al., 2011; Guinan, 2011). Several lines of evidence have demonstrated that the  
89 MOC system has an important role in the protection from NIHL: 1) stimulation of MOC fibers  
90 during sound overexposure produces a reduction of sensitivity loss (Reiter and Liberman, 1995);  
91 2) chronic sectioning of the olivocochlear bundle renders the ear more vulnerable to permanent  
92 acoustic injury (Handrock and Zeisberg, 1982; Kujawa and Liberman, 1997; Maison et al., 2013)  
93 3) the strength of the olivocochlear reflex is inversely correlated with the degree of NIHL

94 (Maison and Liberman, 2000) and 4) genetically modified mice where the magnitude and  
95 duration of efferent cholinergic effects are increased, exhibit higher tolerance to noise-induced  
96 trauma (Taranda et al., 2009). However, the precise role of the MOC reflex on HHL remains  
97 mostly undefined. Recent studies show enhanced cochlear synaptopathy after olivocochlear  
98 bundle lesion, which removes much of the MOC innervation to OHCs with almost no alteration  
99 in the lateral olivocochlear (LOC) neurons (Maison et al., 2013). A variety of data indicate that  
100 MOC neurons release not only acetylcholine but also gamma-aminobutyric acid and calcitonin-  
101 gene related peptide (Maison et al., 2003; Wedemeyer et al., 2013). Thus, cochlear de-  
102 efferentiation produced by surgical lesion to the olivocochlear pathway removes all the different  
103 neurotransmitter/neuromodulator components and possibly some LOC neurons. Here we  
104 explored the effect of the strength of the cholinergic component of the MOC reflex on the  
105 cochlear synaptopathy that occurs in HHL by using genetically modified mice with different  
106 levels of  $\alpha 9\alpha 10$  nAChR activity. In addition, we analyzed for the first time the effect of acoustic  
107 trauma in ears exposed at sound levels well below those that cause hair cell damage and  
108 permanent threshold shifts on efferent synaptic terminals contacting the OHCs. We used mice  
109 at the early onset of puberty, i.e. at three weeks of age, a period of enhanced sensitivity to NIHL  
110 (Henry, 1984; Ohlemiller et al., 2000; Kujawa and Liberman, 2006). Our results show that the  
111 degree of cochlear synaptopathy is negatively correlated to the level of  $\alpha 9\alpha 10$  nAChR activity.  
112 Notably, enhancement of cholinergic activity not only prevented cochlear synaptopathy but also  
113 promoted new afferent synapse formation after acoustic trauma. Moreover, exposure to loud  
114 noise produced plastic changes leading to degeneration of MOC terminals synapsing on OHCs.  
115 We propose that both cochlear synaptopathy and the loss of MOC terminals contribute to HHL,  
116 compromising the performance of complex listening tasks such as understanding speech in a  
117 noisy environment. Therefore, our findings unequivocally show that strengthening of the MOC  
118 feedback by enhancement of  $\alpha 9\alpha 10$  nAChRs activity can prevent the development of HHL

119 symptoms

after

noise

exposure.



120 **Materials and Methods**

121 **Animals.** *Chrna9* KO and *Chrna9*<sup>L9'T</sup> KI mice have been previously described (Vetter et al.,  
122 1999; Taranda et al., 2009) and were backcrossed with congenic FVB.129P2-*Pde6bb* *Tyrc-*  
123 *ch/AntJ* strain (<https://www.jax.org/strain/004828>, RRID:IMSR\_JAX:004828) for seventeen  
124 generations (i.e., N-17). We used a similar male/female ratio in all the experimental groups in  
125 the different genotypes. All experimental protocols were performed in accordance with the  
126 American Veterinary Medical Association (AVMA) Guidelines for the Euthanasia of Animals  
127 (June 2013) as well as Instituto de Investigaciones en Ingeniería Genética y Biología Molecular  
128 (INGEBI) Institutional Animal Care and Use Committee (IACUC) guidelines, and best practice  
129 procedures.

130

131 **Cochlear function tests.** Inner ear physiology, including auditory brainstem responses (ABRs)  
132 and distortion-product otoacoustic emissions (DPOAEs), was performed in mice of either sex  
133 anesthetized with xylazine (10 mg/kg, i.p.) and ketamine (100 mg/kg, i.p.) and placed in a  
134 soundproof chamber maintained at 30°C. The first recording was performed at postnatal day 21  
135 (P21), followed by noise exposure and the additional measurements 1, 7, 8 and 14 days post-  
136 exposure. Sound stimuli were delivered through a custom acoustic system with two dynamic  
137 earphones used as sound sources (CDMG15008-03A; CUI) and an electret condenser  
138 microphone (FG- 23329-PO7; Knowles) coupled to a probe tube to measure sound pressure  
139 near the eardrum (for details, see  
140 [https://www.masseyeandear.org/research/otolaryngology/investigators/laboratories/eaton-](https://www.masseyeandear.org/research/otolaryngology/investigators/laboratories/eaton-peabody-laboratories/epl-engineering-resources/epl-acoustic-system)  
141 [peabody-laboratories/epl-engineering-resources/epl-acoustic-system](https://www.masseyeandear.org/research/otolaryngology/investigators/laboratories/eaton-peabody-laboratories/epl-engineering-resources/epl-acoustic-system)). Digital stimulus  
142 generation and response processing were handled by digital I-O boards from National  
143 Instruments driven by custom software written in LabVIEW (generously given by Dr. M. Charles  
144 Liberman, Eaton-Peabody Laboratories, Massachusetts Eye & Ear Infirmary, Boston, MA.). For

145 ABRs, needle electrodes were placed into the skin at the dorsal midline close to the neural crest  
146 and pinna with a ground electrode near the tail. ABR potentials were evoked with 5 ms tone pips  
147 (0.5 ms rise-fall, with a  $\cos^2$  envelope, at 40/s) delivered to the eardrum at log-spaced  
148 frequencies from 5.6 to 45.25 kHz. The response was amplified 10,000X with a 0.3–3 kHz  
149 passband. Sound level was raised in 5 dB steps from 20 to 80 dB sound pressure level (SPL).  
150 At each level, 1024 responses were averaged with stimulus polarity alternated. Threshold for  
151 ABR was defined as the lowest stimulus level at which a repeatable peak 1 could be identified in  
152 the response waveform. The ABR peak 1 amplitude was computed by off-line analysis of the  
153 peak to baseline amplitude of stored waveforms. The DPOAEs in response to two primary tones  
154 of frequency  $f_1$  and  $f_2$  were recorded at  $2f_1-f_2$ , with  $f_2/f_1=1.2$ , and the  $f_2$  level 10 dB lower than  
155 the  $f_1$  level. Ear-canal sound pressure was amplified and digitally sampled at 4  $\mu$ s intervals.  
156 DPOAE threshold was defined as the lowest  $f_2$  level in which the signal to noise floor ratio is  $>1$ .

157

158 **Noise exposure.** Animals were exposed under anesthesia to a 1-16 kHz noise at 100 dB SPL  
159 for 1 h in the same acoustic chamber used for cochlear function tests. Noise calibration to target  
160 SPL was performed immediately before each acoustic overexposure.

161

162 **Cochlear processing and immunostaining.** For the immunolabeling and quantification we  
163 divided animals for each genotype in two groups: 'Control' and 'seven days after acoustic  
164 trauma (AT + 7d)'. First, we tested the auditory function at P21 in both 'Control' and 'AT + 7d'  
165 groups. Immediately after, the control group was introduced in the acoustic chamber under  
166 anesthesia for 1 hour for a 'sham' condition while the 'AT + 7d' group was exposed to 100 dB  
167 SPL for 1 hour in the same chamber. Acoustic thresholds in both groups were measured again  
168 at one and seven days post-acoustic trauma and after the final auditory test (postnatal day 28),  
169 tissues were collected for immunostaining. Cochleae were perfused intralabyrinthally with 4%  
170 paraformaldehyde (PFA) in phosphate-buffered saline (PBS), post-fixed with 4% PFA overnight,

171 and decalcified in 0.12 M EDTA. Cochlear tissues were then microdissected and permeabilized  
172 by freeze/thawing in 30% sucrose (for CtBP2/GluA2 immunostaining) or directly blocked (for  
173 synaptophysin immunostaining). The microdissected pieces were blocked in 5% normal goat  
174 serum with 1% Triton X-100 in PBS for 1 h, followed by incubation in primary antibodies (diluted  
175 in blocking buffer) at 37°C for 16 h (for CtBP2/GluA2 immunostaining) or 4°C for 16 h (for  
176 synaptophysin immunostaining). The primary antibodies used in this study were: 1) mouse anti-  
177 synaptophysin antibody (Millipore, Billerica, MA; MAB5258, RRID:AB\_2313839, 1:1000) to  
178 reveal the efferent terminals 2) anti-C-terminal binding protein 2 (mouse anti-CtBP2 IgG1; BD  
179 Biosciences, San Jose, CA; #612044, RRID:AB\_399431, 1:200) to label the presynaptic ribbon  
180 and 3) anti-glutamate receptor 2 (mouse anti-GluA2 IgG2a; Millipore, Billerica, MA; MAB397,  
181 RRID:AB\_11212990, 1:2000) to label the post-synaptic receptor plaques. Tissues were then  
182 incubated with the appropriate Alexa Fluor-conjugated fluorescent secondary antibodies  
183 (Invitrogen, Carlsbad, CA; 1:1000 in blocking buffer) for 2 h at room temperature (for  
184 CtBP2/GluA2 immunostaining) or processed with biotinylated secondary, ABC reagent (Vector  
185 Labs, Burlingame, CA, RRID:AB\_2336827), and diaminobenzidine for standard light microscopy  
186 (for synaptophysin immunostaining). Finally, tissues were mounted on microscope slides in  
187 FluorSave mounting media (Millipore, Billerica, MA). For IHCs synaptic counts, confocal z-  
188 stacks (0.1  $\mu\text{m}$  step size) of the apical, medial and basal regions from each cochlea were taken  
189 using a Leica TCS SPE microscope equipped with 63X (1.5X digital zoom) oil-immersion lens.  
190 Image stacks were imported to Fiji software (RRID:SCR\_002285) (Schindelin et al., 2012),  
191 where IHCs were identified based on their CtBP2-stained nuclei. Each image usually contained  
192 10 to 20 IHCs. For each stack, a custom Fiji plugin was developed to automatize the  
193 quantifications of synaptic ribbons, glutamate receptor patches and co-localized synaptic puncta.  
194 Briefly, each channel was analyzed separately and maximum projections were generated to  
195 quantify the number of CtBP2 or GluA2 puncta. Additionally, a composite between the two  
196 channels was produced to draw the different ROIs that correspond to each IHC taking the

197 CtBP2 stained nuclei as a reference. The maximum projections from the single channels were  
198 multiplied to generate a merged 32-bit image of the two channels. Then, they were converted to  
199 binary images after a custom thresholding procedure. Automatic counting of the number of  
200 particles on each ROI was performed.

201

#### 202 **Statistical analysis**

203 Data were analyzed with R Statistical Software (RRID:SCR\_001905). Shapiro-Wilks test was  
204 used for testing normal distribution of the residuals. We used non-parametric tests because our  
205 data were non-normally distributed. For one-group comparisons that involved repeated  
206 measures (ABRs thresholds, peak 1 amplitudes and latencies and DPOAEs thresholds)  
207 Friedman tests were used followed by a post-hoc test (Pohlert, 2014). For group comparisons  
208 that do not involve repeated measures (ABR comparisons of unexposed animals, IHCs synaptic  
209 counts), Kruskal-Wallis non-parametric ANOVA followed by a Dunn's post-tests were used to  
210 determine statistical significance. For independent, two-group comparisons (MOC terminals per  
211 OHC), two-sample Kolmogorov-Smirnov test was applied. Statistical significance was set to  
212  $p < 0.05$ .

213

214 **Results**215 **Auditory function in mice with different degrees of efferent inhibition after acoustic**  
216 **trauma**

217 In order to evaluate cochlear function we recorded ABR, the sound-evoked potentials generated  
218 by neuronal circuits in the ascending auditory pathways. We used genetically modified mice with  
219 different levels of  $\alpha 9\alpha 10$  nAChR activity: *Chrna9* KO mice which lacks cholinergic transmission  
220 between MOC neurons and hair cells (Vetter et al., 1999), and a gain of function *Chrna9L9<sup>T</sup>* KI  
221 mice carrying an  $\alpha 9$  point mutation that leads to enhanced responses to MOC activity (Taranda  
222 et al., 2009). We examined ABR responses at P21 in WT, *Chrna9* KO and *Chrna9L9<sup>T</sup>* KI  
223 unexposed mice and found no difference in the median ABR thresholds between WT and  
224 *Chrna9* KO mice except at the highest frequency tested (Kruskal-Wallis test,  $df=2$ ,  $p=0.04$  at  
225 45.25 kHz). However, median ABR thresholds were slightly elevated by 5 to 10 dB in  
226 *Chrna9L9<sup>T</sup>* KI mice at all the frequencies, except for high frequency stimuli (Kruskal-Wallis test,  
227  $df=2$ ,  $p<0.05$  at 5.6, 8, 11.33 and 16 kHz) (Figure 1a). ABRs peak 1 amplitudes at 80 dB, the  
228 summed activity of the cochlear nerve, were not modified in the three genotypes (Kruskal-Wallis  
229 test,  $df=2$ ,  $p>0.05$  at all the frequencies tested) (Figure 1b).

230 We then exposed WT, *Chrna9* KO and *Chrna9L9<sup>T</sup>* KI mice to a 1-16 kHz noise at 100 dB SPL  
231 for 1 h and tested the animals one and seven days post acoustic trauma (Figure 2). As shown in  
232 Figure 2b, large auditory threshold shifts from 10 to 35 dB SPL were found one day after  
233 exposure in WT and *Chrna9* KO mice (Friedman test,  $df=2$   $p<0.05$  at all the frequencies tested  
234 for both genotypes). One week later, auditory thresholds returned to pre-exposure values in WT  
235 (Friedman test,  $df=2$ ,  $p>0.05$  at all the frequencies tested), a result known to occur in mice with  
236 clear signs of HHL (Kujawa and Liberman, 2009). However, in *Chrna9* KO ears, which lack a  
237 functional MOC system feedback, auditory thresholds did not recover (Friedman test,  $df=2$ ,  
238  $p<0.05$  at all the frequencies tested), indicating a persistence of damage (Figure 2b, middle

239 panel). In contrast, the *Chrna9L9'T* KI gain-of-function mouse model with an enhanced  $\alpha 9\alpha 10$   
240 nAChRs activity was completely resistant to the same acoustic exposure protocol (Friedman  
241 test,  $df=2$ ,  $p>0.05$  at all the frequencies tested) (Figure 2b, right panel).

242 One signature of cochlear synaptopathy observed in HHL in mice is a reduction of ABR peak 1  
243 amplitudes without permanent changes in ABR thresholds (Kujawa and Liberman, 2009). This  
244 peak represents the summed sound-evoked spike activity at the first synapse between IHCs  
245 and afferent nerve fibers (Buchwald and Huang, 1975; Antoli-Candela and Kiang, 1978). As  
246 shown in Figure 2a and c, a large reduction in amplitudes were observed at 11.33, 16 and 22.65  
247 kHz in WT mice one day after acoustic trauma (Friedman test,  $df=2$ ,  $p=0.048$  at 11.33 kHz;  
248  $p=0.026$  at 16 kHz and  $p=0.018$  at 22.65 kHz), which did not completely recover after seven  
249 days (Friedman test,  $df=2$ ,  $p=0.048$  at 16 kHz and  $p=0.003$  at 22.65 kHz). Similarly, in *Chrna9*  
250 KO mice, ABR peak 1 amplitudes were reduced one day after trauma at 5.6, 16, 22.65 and 32  
251 kHz (Friedman test,  $df=2$ ,  $p=0.048$  at 5.6 kHz;  $p=0.007$  at 16 kHz;  $p=0.01$  at 22.65 kHz and  
252  $p=0.026$  at 32 kHz). Seven days after acoustic overexposure ABR peak 1 amplitudes did not  
253 completely recover, however, it was not significantly different (Friedman test,  $df=2$ ,  $p>0.05$  at all  
254 the frequencies tested) (Figure 2a and c). Interestingly, ABR peak 1 amplitudes were not  
255 modified in the *Chrna9L9'T* KI mice after acoustic trauma (Friedman test,  $df=2$ ,  $p>0.05$  at all the  
256 frequencies tested), suggesting that enhanced  $\alpha 9\alpha 10$  nAChRs activity might prevent the loss of  
257 afferent synapses. The ABR peak 1 latencies were not altered after acoustic trauma in any of  
258 the evaluated genotypes (Friedman test,  $df=2$   $p<0.05$  at all the frequencies tested for all the  
259 genotypes) (Figure 2d), indicating that variation in the MOC strength does not affect the  
260 conduction velocity of cochlear nerve fibers.

261

262 **Noise-induced cochlear synaptopathy in mice with different levels of MOC feedback**

263 Cochleae were harvested and fixed for histological analysis at P28 in all the different groups.  
264 Hair cell count showed no loss of IHCs or OHCs in the different genotypes in controls and  
265 exposed groups (data not shown). To analyze the IHCs-auditory nerve fibers synapses, organ  
266 of Corti whole-mounts were immunostained with antibodies against CtBP2-Ribeye, a critical  
267 protein present at the presynaptic ribbon (Khimich et al., 2005) and GluA2 AMPA-type  
268 glutamate receptors, which are expressed at the postsynaptic afferent terminal (Matsubara et al.,  
269 1996; Liberman et al., 2011; Maison et al., 2013). IHC-afferent synapses were identified by  
270 colocalization of a pair of CtBP2/GluA2 puncta at the base of the IHC (Liberman et al., 2011). In  
271 each whole mount organ of Corti, counting was done at three different cochlear locations: apical,  
272 medial and basal. The number of pre, post or colocalized synaptic markers was averaged from  
273 10 to 20 IHCs per each imaged cochlear section (4 to 14 animals per genotype) to generate the  
274 synaptic density per IHC.

275 First, we compared the number of pre, post and colocalized synaptic markers per IHC in  
276 unexposed WT, *Chrna9* KO and *Chrna9L9'T* KI mice (Figure 3). Synaptic counts were lower in  
277 *Chrna9* KO compared to WT mice in the apical cochlear end (Kruskal-Wallis test, apical:  
278  $\chi^2=17.4$ ,  $df=1$ ,  $p<0.001$ ) (Figure 3, right panel). However, there was a slight, but significant  
279 increase in the number of ribbon synapses in the medial cochlear region (Kruskal-Wallis test;  
280 medial:  $\chi^2=6.1$ ,  $df=1$ ,  $p=0.01$ ) (Figure 3, right panel). It is important to note that synaptic counts  
281 showed the same spatial distribution in *Chrna9* KO compared to WT mice: the number of ribbon  
282 synapses peaks in the medial region where the cochlea is most sensitive to sound (Figure 3).  
283 Nevertheless, in *Chrna9L9'T* KI mice synaptic counts were comparable to WT mice in low and  
284 high frequency areas, but in the middle cochlear region a large reduction in synaptic counts of  
285 around 15% was observed (Kruskal-Wallis test,  $\chi^2=19.3$ ,  $df=1$ ,  $p<0.0001$ ) (Figure 3, right panel).  
286 Thus, the spatial distribution from base to apex seen in WT and *Chrna9* KO ears seems to be  
287 lost in the *Chrna9L9'T* KI mice.

288 The impact of noise exposure on the number of auditory nerve synapses is summarized in  
289 Figure 4. Ribbon (CtBP2) counts in WT exposed ears were significantly reduced in the three  
290 cochlear regions (Figure 4a). Reduction was more pronounced in the low (apical-end) and high  
291 (basal-end) frequency regions with a 10% reduction compared to controls (Kruskal-Wallis test;  
292 apical:  $\chi^2=23.6$ ,  $df=1$ ,  $p<0.0001$  and basal:  $\chi^2=8.9$ ,  $df=1$ ,  $p=0.002$ ). Similarly, GluA2 postsynaptic  
293 receptors were diminished in the whole cochlea of traumatized WT mice with a bigger reduction  
294 at the apical and medial turns (Kruskal-Wallis test; apical:  $\chi^2=42.2$ ,  $df=1$ ,  $p<0.0001$  and medial:  
295  $\chi^2= 5.8$ ,  $df=1$ ,  $p=0.01$ ). Putative ribbon synapse counts, defined as juxtaposed CtBP2- and  
296 GluA2-positive puncta showed a 10% reduction only in the apical turn after acoustic trauma in  
297 WT mice (Kruskal-Wallis test,  $\chi^2=26.4$ ,  $df=1$ ,  $p< 0.0001$ ) (Figure 4a, right panel).

298 In *Chrna9* KO mice there was also a reduction in the number of pre, post and colocalized  
299 puncta, depending on cochlear frequency/location after exposure to noise (Figure 4b). Ribbon  
300 puncta in *Chrna9* KO exposed ears were reduced up to a 20% of the control at the basal  
301 cochlear end after acoustic trauma (Kruskal-Wallis test,  $\chi^2=53.8$ ,  $df=1$ ,  $p<0.0001$ ). GluA2  
302 postsynaptic receptors were reduced by 13% in both the apical and basal turns of traumatized  
303 mice (Kruskal-Wallis test; apical:  $\chi^2=25.4$ ,  $df=1$ ,  $p<0.0001$  and basal:  $\chi^2=24.4$ ,  $df=1$ ,  $p<0.0001$ ).  
304 Synaptic puncta showed a 20% reduction only in the basal turn after acoustic trauma (Kruskal-  
305 Wallis test,  $\chi^2=41.7$ ,  $df=1$ ,  $p<0.0001$ ) (Figure 4b, right panel).

306 Surprisingly, after seven days of acoustic exposure, higher density (approximately 10-15%  
307 increase) of pre-synaptic ribbons, post-synaptic GluA2 receptor patches, and putative synapses  
308 at all cochlear regions were observed in *Chrna9L9'T* KI ears (Figure 4c) (synaptic counts,  
309 Kruskal-Wallis test; apical:  $\chi^2=14.9$ ,  $df=1$ ,  $p=0.0001$ , medial:  $\chi^2=64.8$ ,  $df=1$ ,  $p<0.0001$  and basal:  
310  $\chi^2=6.7$ ,  $df=1$ ,  $p=0.009$ ) (Figure 4c, right panel). These results suggest that potentiation of  $\alpha 9\alpha 10$



311 nAChRs responses can not only prevent the noise-induced functional signs of HHL and afferent  
312 synaptic loss but also might promote synapse formation after acoustic trauma.

313

#### 314 **OHC function and efferent innervation pattern after noise exposure**

315 OHC function was assessed through DPOAEs, which can be measured from the external  
316 auditory canal (Shera and Guinan, 1999). When two tones are presented, electrical distortions  
317 are created, amplified and conducted back into mechanical motion of the sensory epithelium at  
318 the distortion frequencies by normally functioning OHCs and can be detected by a microphone  
319 in close proximity to the tympanic membrane. As shown in Figure 1c, DPOAEs responses at  
320 P21 in unexposed WT and *Chrna9* KO mice were similar except at 45.25 kHz (Kruskal-Wallis  
321 test,  $df=2$ ,  $p=0.004$  at 45.25 kHz). However, there was a small elevation of around 5 dB of mean  
322 DPOAEs thresholds in unexposed *Chrna9L9'T* KI mice at some frequencies (Kruskal-Wallis test,  
323  $\chi^2=7.3$ ,  $df=2$ ,  $p=0.020$  at 11.33 kHz;  $\chi^2=5.7$ ,  $df=2$ ,  $p=0.004$  at 16 kHz and  $\chi^2=10.8$ ,  $df=2$ ,  $p=0.030$   
324 at 22.65 kHz) (Figure 1c). Threshold elevations in *Chrna9L9'T* KI mice were similar in  
325 magnitude whether measured by ABRs (Figure 1a) or DPOAEs (Figure 1c), as already reported  
326 by Taranda et al. 2009. Thus, compared to *Chrna9* KO mice, in which baseline cochlear  
327 thresholds were normal, elevated thresholds in unexposed *Chrna9L9'T* KI mice suggest that  
328 they may arise from the enhancement of cholinergic activity on OHCs, revealing cholinergic  
329 MOC effects under resting conditions. However, we cannot disregard that unexposed  
330 *Chrna9L9'T* KI mice have fewer afferent synapses per IHC at the medial cochlear region (Figure  
331 3) and this may also contribute to generating higher auditory thresholds in these mice.

332 In WT ears, with normal MOC feedback, exposure to loud sounds produced DPOAEs threshold  
333 shifts from 5 to 20 dB one day after acoustic trauma at some frequencies (Friedman test,  $df=2$ ,  
334  $p=0.019$  at 11.33 kHz;  $p=0.012$  at 16 kHz;  $p=0.001$  at 22.65 kHz and  $p=0.012$  at 32 kHz) that  
335 returned to almost normal at day 7 (Friedman test,  $df=2$ ,  $p>0.05$  at all the frequencies tested)

336 (Figure 5, left panel). In contrast, in *Chrna9* KO mice, which are functionally de-efferented, noise  
337 exposure produced DPOAEs threshold shifts from 5 to 35 dB one day after trauma at some  
338 frequencies (Friedman test,  $df=2$ ,  $p= 0.022$  at 11.33 kHz;  $p=0.003$  at 16 kHz;  $p= 0.017$  at 22.65  
339 kHz;  $p=0.014$  at 32 kHz and  $p=0.014$  at 45.25 kHz). DPOAEs thresholds remained elevated for  
340 at least seven days after exposure (Friedman test,  $df=2$ ,  $p=0.009$  at 11.33 kHz;  $p=0.009$  at 16  
341 kHz;  $p=0.030$  at 22.65 kHz;  $p=0.014$  at 32 kHz and  $p=0.043$  at 45.25 kHz) (Figure 5, middle  
342 panel). Remarkably, there were no changes in DPOAEs thresholds after acoustic trauma in  
343 *Chrna9L9'T* KI mice with enhanced MOC feedback (Friedman test,  $df=2$ ,  $p>0.05$  at all the  
344 frequencies tested) (Figure 5, right panel). These results show that the degree of functional  
345 OHC damage depends on the level of  $\alpha 9\alpha 10$  nAChRs activity.

346 In order to evaluate if exposure to loud sounds can alter the distribution of MOC terminals in  
347 OHCs, a quantitative analysis of whole mount organ of Corti immunostained for synaptophysin,  
348 an integral protein of the synaptic vesicle membrane, was performed (Figure 6). In WT mice,  
349 MOC terminals typically occur in clusters under OHCs, along the entire cochlea from base to  
350 apex (Vetter et al., 1999). As seen in Figure 6b, left panel, in the middle cochlear turn, the  
351 number of terminals per OHC in WT ranged from 1 to 5, with most of the OHCs contacted by 2  
352 to 3 synaptic terminals (39.8 and 41.7 %, respectively). However, seven days after acoustic  
353 trauma there was a reduction in the number of MOC terminals per OHC with almost 40% of  
354 terminals occurring as singlets rather than as clusters. The mean number of terminals under  
355 OHCs before and 7 days after acoustic overexposure was reduced from  $2.60 \pm 0.02$  to  $1.80 \pm$   
356  $0.01$ , respectively. Thus, the distribution of MOC contacts under OHC was significantly changed  
357 after noise exposure (two-sample Kolmogorov-Smirnov test,  $D=0.3$ ,  $p<0.0001$ ).

358 As previously reported (Vetter et al., 1999), quantification of MOC endings in cochlear sections  
359 of *Chrna9* KO mice revealed abnormalities in the number of terminals. Most OHCs were  
360 contacted by 1 to 2 terminals (39.3 and 52.4 %, respectively) and very few by more than 2. After

361 acoustic trauma, there were no changes in the pattern of labeled terminals in *Chrna9* KO mice  
362 (Figure 6a and b, middle panels). In contrast, the *Chrna9L9'T* KI gain-of-function mouse model  
363 already showed a basal increase in the mean number of efferent terminals per OHC, with some  
364 cells contacted by as many as 7 terminals (Figure 6a, right panel). Previous studies in  
365 *Chrna9L9'T* KI mice have shown the same increase in the mean number of efferent terminals  
366 per OHC (Murthy et al., 2009). Notably, no changes were observed in the number and  
367 distribution of efferent terminals under OHCs in the *Chrna9L9'T* KI mice after exposure to loud  
368 sounds (Figure 6a and b, right panels). Altogether, these observations suggest that  $\alpha 9\alpha 10$   
369 nAChR activity influences olivocochlear pre-synaptic terminal differentiation required for proper  
370 synapse assembly.

371 Although healthy adult IHCs lack MOC innervation, it has been recently suggested that MOC  
372 contacts return to IHCs in the damaged and aged cochlea (Ruel et al., 2007; Lauer et al., 2012;  
373 Zachary and Fuchs, 2015). To determine if the present noise exposure protocol can produce  
374 changes in MOC synapses on IHCs we analyzed synaptophysin-stained cochlea in the IHCs'  
375 area. Figure 6c shows light microscopy micrographs of the inner spiral bundle that reveal the  
376 olivocochlear innervation. Synaptophysin labels both MOC and LOC fibers, which cannot be  
377 differentiated. As previously demonstrated by Vetter et al., 1999, in unexposed WT mice the  
378 spiraling plexus of efferent terminals consist of a dense matrix at levels well below the IHC base,  
379 on the modiolar side, where terminals contact dendrites of auditory nerve fibers. Moreover, a  
380 sporadic plexus of terminals positioned around the IHC soma on the pillar side was observed  
381 (Figure 6c, top left panel, arrowheads). Seven days after noise exposure there was no apparent  
382 change in the efferent terminals of the IHCs area (Figure 6c, bottom left panel). Thus, similar to  
383 unexposed ears, the dense matrix of efferent terminals at the base of the IHCs showed no  
384 alteration and a much sparser innervation in the IHC somata region was observed. Interestingly,  
385 as previously shown (Vetter et al., 1999), under control conditions the population of efferent

386 terminals on the pillar side of IHCs appears to be absent in *Chrna9* KO mice, whereas the  
387 terminals on the modiolar side was not modified (Figure 6c, upper middle panel). After acoustic  
388 trauma, there was no overt change in the pattern of labeled terminals in *Chrna9* KO mice  
389 (Figure 6C, lower middle panel). Finally, in the organ of Corti of unexposed *Chrna9L9<sup>+</sup>T* KI mice,  
390 synaptophysin immunostaining revealed an intense cholinergic innervation (Figure 6c, upper  
391 right panel) with an apparent increase in the number of terminals in the pillar side. Furthermore,  
392 efferent terminals appeared disorganized compared to WT mice. Seven days after acoustic  
393 overexposure, there was no overt change in the pattern of efferent innervation in *Chrna9L9<sup>+</sup>T* KI  
394 mice (Figure 6c, lower right panel).

395 The reduction in the number of efferent contacts in WT OHCs after noise exposure (Figure 6a  
396 and b, left panels) led us to analyze if further de-efferentation would occur when applying a  
397 second noise challenge of 1h at 100 dB SPL, that could render the organ of Corti totally devoid  
398 of efferent feedback. At P28 (i.e., seven days after the first noise exposure), we exposed WT  
399 again and tested their cochlear function the next day and seven days after. This second  
400 exposure caused the same ABR threshold elevations one day post acoustic trauma (Friedman  
401 test,  $df=4$ ,  $p=0.0375$  at 11.33 kHz;  $p=0.016$  at 16 kHz;  $p=0.049$  at 22.65 kHz;  $p=0.009$  at 32 kHz  
402 and  $p=0.022$  at 45.25 kHz), which completely recovered to pre-exposure values by seven days  
403 after the second noise challenge (Friedman test,  $df=4$ ,  $p>0.05$  at all the frequencies tested)  
404 (Figure 7a). The distribution pattern of MOC terminals in the OHC area, analyzed by  
405 synaptophysin immunostaining, showed no further de-efferentation (Figure 7b). The mean  
406 number of MOC terminals under OHCs after the first and second acoustic overexposure was  
407  $1.80 \pm 0.01$  and  $2.09 \pm 0.01$ , respectively. These results suggest that with a consecutive noise  
408 exposure there is no additional degeneration of MOC terminals and that their cochlear  
409 sensitivity was not altered.

410

411 **Discussion**

412 HHL was recently described as an auditory neuropathy believed to contribute to perceptual  
413 abnormalities including tinnitus, hyperacusis and speech discrimination in noisy environments  
414 (Kujawa and Liberman, 2009; Schaette and McAlpine, 2011). The causative contribution of  
415 cochlear synaptopathy to HHL has become the most suitable explanation since in the noise-  
416 exposed and/or aging ear significant IHC de-afferentation takes place well before elevation of  
417 auditory thresholds (Kujawa and Liberman, 2009). Here we show an inverse correlation  
418 between activity of the  $\alpha 9\alpha 10$  nAChRs and the HHL phenotype, which is suggestive of the  
419 critical role of the MOC system in cochlear synaptopathy.

420 Until now, delivery of neurotrophins appeared as the only way of triggering the repair of noise-  
421 induced damage to cochlear synapses (Wan et al., 2014; Suzuki et al., 2016). Our study shows  
422 that enhancement of the MOC feedback can counteract noise-induced cochlear synaptopathy  
423 and the loss of MOC terminals. Thus, potentiation of  $\alpha 9\alpha 10$  nAChR-mediated responses by a  
424 pharmacological positive modulator could have a potential therapeutic use in the prevention or  
425 treatment of HHL.

426

427 **Noise-induced cochlear synaptopathy and MOC feedback**

428 Noise-induced cochlear synaptopathy was initially described in adult mice with an up to 40% of  
429 synaptic loss (Kujawa and Liberman, 2009) and afterwards validated in guinea pigs with a  
430 smaller reduction of 30% (Furman et al., 2013). A more recent study in mice revealed a similar  
431 degree of cochlear synaptopathy at 6 weeks of age (Jensen et al., 2015). Similarly, in aging  
432 mice, there is a 25-30% loss of cochlear nerve synapses, well before there is any loss of hair  
433 cells or significant threshold elevation (Sergeyenko et al., 2013). Our work shows noise-induced  
434 cochlear synaptopathy at P21, i.e. just at the early onset of puberty and also an early stage of  
435 the development of the hearing system. The smaller reduction in our ribbon synapses counts  
436 (up to 20%) compared to that described by Kujawa and Liberman (2009) can derive from

437 differences in mice strains and/or from a reduced time of the noise exposure protocol. Although  
438 most studies have been performed in rodents, a recent work has described noise-induced loss  
439 of ribbon synapses in non-human primates (Valero et al., 2017). Several lines of evidence  
440 indicate that humans are less vulnerable to noise injury (Dobie and Humes, 2017). Nonetheless,  
441 emerging information in humans show that auditory nerve fibers are more susceptible than hair  
442 cells, as in rodents (Viana et al., 2015). Taken together, these results suggest that cochlear  
443 synaptopathy is a general phenomenon that occurs in different species and at different stages  
444 of development and might be a more important factor in noise-induced and age-related hearing  
445 loss than previously valued.

446 It has been proposed that the MOC reflex in adults controls the dynamic range of hearing  
447 (Guinan, 1996), improves signal detection in background noise (Kawase et al., 1993), is  
448 involved in selective attention (Delano et al., 2007), and protects from acoustic injury (Liberman,  
449 1991). Before hearing onset, MOC neurons establish transient synapses on IHCs somata  
450 mediated by  $\alpha 9\alpha 10$  nAChRs (Glowatzki and Fuchs, 2000; Katz et al., 2004; Gómez-Casati et al.,  
451 2005). This transient MOC activity modulates the temporal fine structure of spontaneous activity  
452 and plays a role in the maturation of the IHC synaptic machinery and central synapse formation  
453 (Glowatzki and Fuchs, 2002; Johnson et al., 2013; Clause et al., 2014). However, the  
454 importance of the MOC system on the maintenance of cochlear nerve synapses after damage  
455 has not been deeply studied. Recent work in mice with cochlear de-efferentation induced by  
456 surgical lesion, showed a dramatic loss of ribbon synapses after exposure to noise (Maison et  
457 al., 2013). Although the surgery spares most of the LOC neurons, some of them can be affected.  
458 The present work provides evidence that MOC-mediated protection of cochlear synaptopathy is  
459 via the  $\alpha 9\alpha 10$  nAChRs complexes on OHCs. However, a developmental effect of an altered  
460  $\alpha 9\alpha 10$  nAChRs activity on the susceptibility to damage in IHCs and auditory nerve fibers cannot  
461 be precluded. The magnitude of cochlear synaptopathy is inversely correlated with the activity of

462  $\alpha 9\alpha 10$  nAChRs: high in *Chrna9* KO and undetectable in *Chrna9L9'T* KI mice. Previous work  
463 with *Chrna9L9'T* KI mice showed that increasing the magnitude of MOC effects rendered mice  
464 more resistant to acoustic trauma (Taranda et al., 2009). This is consistent with studies showing  
465 that overexpressing the  $\alpha 9$  channels also increased the resistance of the ear to noise injury  
466 (Maison et al., 2002). We now show that the enhanced  $\alpha 9\alpha 10$  nAChRs activity also prevents  
467 cochlear synaptopathy and points to the importance of the integrity of MOC synapses as a  
468 feedback pathway to protect the inner ear from everyday acoustic environments.

469 The reduction in synaptic counts can account for the decrease in neural response amplitudes  
470 after acoustic trauma in WT and *Chrna9* KO mice. A decrease in the number of ribbon synapses  
471 could reduce the amount of synchronous excitatory postsynaptic potentials in response to  
472 sounds altering the amplitude of ABR peak 1 (Kiang et al., 1976; Kujawa and Liberman, 2009).  
473 It will be interesting to investigate if the remaining synapses are equally capable of releasing  
474 glutamate as before trauma. Similarly, the lack of reduction in ABR amplitudes in *Chrna9L9'T* KI  
475 mice correlates with the absence of synaptic loss after acoustic overexposure, indicating that  
476 enhancement of the MOC reflex prevents the neuronal loss.

477 The observation in *Chrna9L9'T* KI mice of an increase in synaptic counts after noise exposure,  
478 is intriguing. In unexposed WT ears, synaptic counts show a spatial distribution from base to  
479 apex: the number of ribbon synapses per IHC peaks at the medial region, where the cochlea is  
480 most sensitive to sound (Meyer et al., 2009). However, in *Chrna9L9'T* KI this distribution is lost:  
481 synaptic counts were comparable to WT mice at low and high frequency regions, except in the  
482 middle turn where a significant reduction was observed. One possibility to explain the abnormal  
483 cochlear distribution of ribbon synapses in the *Chrna9L9'T* KI mouse model is that before the  
484 onset of hearing, the enhanced transient MOC activity could modify the pattern of spontaneous  
485 IHC firing, leading to an alteration in the definitive number of auditory nerve synapses.  
486 Nevertheless, after acoustic trauma there was an increase in synaptic puncta across the

487 cochlea suggesting that enhancement of MOC activity together with sound overexposure  
488 prompted new afferent synapse formation. An alternative explanation may be that the cochlea  
489 already contains synaptic contacts, but without pre- and post-synaptic specializations necessary  
490 for neurotransmission, which then gain function following noise trauma. The functionality of  
491 these new synapses is still an open question, since there were no changes in ABR peak 1  
492 amplitudes in *Chrna9*<sup>L9'T</sup> KI mice after acoustic trauma. Currently, we can speculate that  
493 acoustic overexposure in this gain of function mouse model could lead to longer lasting  
494 increases in intracellular calcium concentration (Wedemeyer et al., 2018) serving as a second  
495 messenger to increase the expression of, for example, neurotrophic factors which might finally  
496 allow the formation of new synapses. Taken together, the present results show for the first time  
497 that potentiation of the MOC system not only strengthens cochlear suppression *in vivo*, but also  
498 triggers cellular and molecular pathways that protect and/or repair the inner ear sensory  
499 epithelium after injury.

500

#### 501 **OHCs function after noise exposure and MOC feedback**

502 DPOAEs threshold measurements show the same inverse correlation between the strength of  
503 MOC activity and the degree of acoustic damage. WT ears presented a transient elevation after  
504 acoustic trauma indicating a full recovery of OHCs function throughout the ear's dynamic range.  
505 In contrast, *Chrna9* KO mice thresholds remain elevated, suggesting OHCs dysfunction after  
506 noise overexposure. It is interesting to note that after acoustic trauma we did not observe any  
507 loss of OHCs in the *Chrna9* KO, suggesting that elevation of DPOAEs thresholds is not caused  
508 by OHCs death. Instead, it could indicate that acoustic overexposure without a functional  
509 inhibitory MOC reflex can alter the OHC electromotility by changing the mechanotransduction  
510 and/or prestin properties. It remains to be shown whether OHCs are more prone to  
511 degeneration in *Chrna9* KO mice after more than a week post-exposure. In agreement with our  
512 observations, it has been shown that cochlear de-efferentation produces permanent DPOAEs



513 threshold elevations without or with minimal OHC loss in aged and noise-exposed mice,  
514 respectively (Maison et al., 2013; Liberman et al., 2014). Conversely, DPOAEs thresholds in  
515 *Chrna9L9<sup>T</sup>* KI mice were not modified with the same noise protocol, showing that enhanced  
516 MOC activity can protect OHCs damage after acoustic overexposure.

517

#### 518 **Noise-induced degeneration of MOC terminals**

519 The present work shows for the first time that noise exposure leading to temporary threshold  
520 shifts and cochlear synaptopathy also causes a reduction of MOC terminals to OHCs. There is a  
521 sparse literature dealing with degeneration of MOC terminals after exposure to noise. Only few  
522 studies have shown acute damage to efferent nerve endings immediately following noise  
523 exposure, but they used an acoustic trauma protocol that causes permanent auditory threshold  
524 elevations concomitantly with OHCs loss in some cochlear regions (Omata et al., 1992; Canlon  
525 et al., 1999). It has been suggested that degeneration of MOC neurons could be a contributing  
526 factor to age-related hearing loss (Liberman et al., 2014; Chumak et al., 2016). However, recent  
527 work by Lauer (2017) with the *Chrna9* KO mice did not find accelerated onset of hearing loss up  
528 to 15 months of age. Considering that MOC neurons regulate several aspects of auditory  
529 processing like the dynamic range of hearing and detection of relevant auditory signals in  
530 background noise (Maison et al., 2001; Guinan, 2011), we propose that the interruption in  
531 synaptic communication between MOC terminals and OHCs after acoustic trauma contributes,  
532 together with cochlear synaptopathy, to the HHL reported symptoms.

533

#### 534 **References**

- 535 Antoli-Candela FJ, Kiang NYS (1978) Unit activity underlying the N1 potential. In: Evoked  
536 electrical activity in the auditory nervous system (Naunton R, Fernandez C, eds), pp 165–  
537 191. New York, NY.
- 538 Ballestero J, Zorrilla de San Martín J, Goutman J, Elgoyhen AB, Fuchs P a, Katz E (2011)

- 539 Short-term synaptic plasticity regulates the level of olivocochlear inhibition to auditory hair  
540 cells. *J Neurosci* 31:14763–14774.
- 541 Beutner D, Moser T (2001) The presynaptic function of mouse cochlear inner hair cells during  
542 development of hearing. *J Neurosci* 21:4593–4599.
- 543 Buchwald JS, Huang C (1975) Far-field acoustic response: origins in the cat. *Science* 189:382–  
544 384.
- 545 Canlon B, Fransson A, Viberg A (1999) Medial olivocochlear efferent terminals are protected by  
546 sound conditioning. *Brain Res* 850:253–260.
- 547 Chumak T, Bohuslavova R, Macova I, Dodd N, Buckiova D, Fritzsich B, Syka J, Pavlinkova G  
548 (2016) Deterioration of the Medial Olivocochlear Efferent System Accelerates Age-Related  
549 Hearing Loss in Pax2-Isl1 Transgenic Mice. *Mol Neurobiol* 53:2368–2383.
- 550 Clause A, Kim G, Sonntag M, Weisz CJC, Vetter DE, RübSamen R, Kandler K (2014) The  
551 precise temporal pattern of prehearing spontaneous activity is necessary for tonotopic map  
552 refinement. *Neuron* 82:822–835.
- 553 Costalupes JA (1985) Representation of tones in noise in the responses of auditory nerve fibers  
554 in cats. I. Comparison with detection thresholds. *J Neurosci* 5:3261–3269.
- 555 Delano PH, Elgueda D, Hamame CM, Robles L (2007) Selective attention to visual stimuli  
556 reduces cochlear sensitivity in chinchillas. *J Neurosci* 27:4146–4153.
- 557 Dobie RA, Humes LE (2017) Commentary on the regulatory implications of noise-induced  
558 cochlear neuropathy. *Int J Audiol* 56:74–78.
- 559 Dolan DF, Nuttall AL (1988) Masked cochlear whole-nerve response intensity functions altered  
560 by electrical stimulation of the crossed olivocochlear bundle. *J Acoust Soc Am* 83:1081–  
561 1086.
- 562 Elgoyhen AB, Johnson DS, Boulter J, Vetter DE, Heinemann S (1994) Alpha 9: an acetylcholine  
563 receptor with novel pharmacological properties expressed in rat cochlear hair cells. *Cell*  
564 79:705–715.

- 565 Elgoyhen AB, Vetter DE, Katz E, Rothlin C V, Heinemann SF, Boulter J (2001)  $\alpha 10$ : a  
566 determinant of nicotinic cholinergic receptor function in mammalian vestibular and cochlear  
567 mechanosensory hair cells. *Proc Natl Acad Sci U S A* 98:3501–3506.
- 568 Fernandez KA, Jeffers PWC, Lall K, Liberman MC, Kujawa SG (2015) Aging after noise  
569 exposure: acceleration of cochlear synaptopathy in “recovered” ears. *J*  
570 *Neurosci* 35:7509–7520.
- 571 Furman AC, Kujawa SG, Liberman MC (2013) Noise-induced cochlear neuropathy is selective  
572 for fibers with low spontaneous rates. *J Neurophysiol* 110:577–586.
- 573 Galambos R (1955) Suppression of auditory nerve activity by stimulation of efferent fibers to  
574 cochlea. *J Neurophysiol* 5:424–437.
- 575 Glowatzki E, Fuchs PA (2000) Cholinergic synaptic inhibition of inner hair cells in the neonatal  
576 mammalian cochlea. *Science* 288:2366–2368.
- 577 Glowatzki E, Fuchs PA (2002) Transmitter release at the hair cell ribbon synapse. *Nat Neurosci*  
578 5:147–154.
- 579 Gómez-Casati ME, Fuchs P a, Elgoyhen AB, Katz E (2005) Biophysical and pharmacological  
580 characterization of nicotinic cholinergic receptors in rat cochlear inner hair cells. *J Physiol*  
581 566:103–118.
- 582 Guinan JJ (1996) Physiology of Olivocochlear Efferents. In: *The Cochlea* (Dallos P, Popper AN,  
583 Fay RR, eds), pp 435–502 Springer Handbook of Auditory Research. New York, NY:  
584 Springer New York.
- 585 Guinan JJ (2011) Physiology of the Medial and Lateral Olivocochlear Systems. In, pp 39–81.
- 586 Handrock M, Zeisberg J (1982) The influence of the efferent system on adaptation, temporary and  
587 permanent threshold shift. *Arch Otorhinolaryngol* 234:191–195.
- 588 Henry KR (1984) Noise and the young mouse: genotype modifies the sensitive period for effects  
589 on cochlear physiology and audiogenic seizures. *Behav Neurosci* 98:1073–1082.
- 590 Jensen JB, Lysaght AC, Liberman MC, Qvortrup K, Stankovic KM (2015) Immediate and

- 591 delayed cochlear neuropathy after noise exposure in pubescent mice. *PLoS One*  
592 10:e0125160.
- 593 Johnson SL, Wedemeyer C, Vetter DE, Adachi R, Holley MC, Elgoyhen AB, Marcotti W (2013)  
594 Cholinergic efferent synaptic transmission regulates the maturation of auditory hair cell  
595 ribbon synapses. *Open Biol* 3:130163.
- 596 Katz E, Elgoyhen AB, Gómez-Casati ME, Knipper M, Vetter DE, Fuchs P a, Glowatzki E (2004)  
597 Developmental regulation of nicotinic synapses on cochlear inner hair cells. *J Neurosci*  
598 24:7814–7820.
- 599 Kawase T, Delgutte B, Liberman MC (1993) Antimasking effects of the olivocochlear reflex. II.  
600 Enhancement of auditory-nerve response to masked tones. *J Neurophysiol* 70:2533–2549.
- 601 Khimich D, Nouvian R, Pujol R, Tom Dieck S, Egnér A, Gundelfinger ED, Moser T (2005) Hair  
602 cell synaptic ribbons are essential for synchronous auditory signalling. *Nature* 434:889–894.
- 603 Kiang NYS, Moxon E., Kahn A. (1976) The relationship of gross potentials recorded from the  
604 cochlea to single unit activity in the auditory nerve. In: *Electrocochleography* (Ruben R.,  
605 Eberling C, Solomon G, eds). Baltimore: University Park.
- 606 Kujawa SG, Liberman MC (1997) Conditioning-related protection from acoustic injury: effects of  
607 chronic deafferentation and sham surgery. *J Neurophysiol* 78:3095–3106.
- 608 Kujawa SG, Liberman MC (2006) Acceleration of age-related hearing loss by early noise  
609 exposure: evidence of a misspent youth. *J Neurosci* 26:2115–2123.
- 610 Kujawa SG, Liberman MC (2009) Adding insult to injury: cochlear nerve degeneration after  
611 “temporary” noise-induced hearing loss. *J Neurosci* 29:14077–14085.
- 612 Lauer AM (2017) Minimal effects of age and exposure to a noisy environment on hearing in  
613 alpha9 nicotinic receptor knockout mice. *Front Neurosci* 11:1–10.
- 614 Lauer AM, Fuchs P a, Ryugo DK, Francis HW (2012) Efferent synapses return to inner hair cells  
615 in the aging cochlea. *Neurobiol Aging* 33:2892–2902.
- 616 Liberman LD, Liberman MC (2015) Dynamics of cochlear synaptopathy after acoustic

- 617 overexposure. *JARO - J Assoc Res Otolaryngol* 16:205–219.
- 618 Liberman LD, Wang H, Liberman MC (2011) Opposing gradients of ribbon size and AMPA  
619 receptor expression underlie sensitivity differences among cochlear-nerve/hair-cell  
620 synapses. *J Neurosci* 31:801–808.
- 621 Liberman M, Mulroy M (1982) New perspectives on noise-induced hearing loss. In (Hamernik R,  
622 Henderson D, Salvi R, eds), pp 105–136. New York, NY.
- 623 Liberman MC (1991) The olivocochlear efferent bundle and susceptibility of the inner ear to  
624 acoustic injury. *J Neurophysiol* 65:123–132.
- 625 Liberman MC, Liberman LD, Maison SF (2014) Efferent feedback slows cochlear aging. *J*  
626 *Neurosci* 34:4599–4607.
- 627 Maison S, Micheyl C, Collet L (2001) Influence of focused auditory attention on cochlear activity  
628 in humans. *Psychophysiology* 38:35–40.
- 629 Maison SF, Adams JC, Liberman MC (2003) Olivocochlear innervation in the mouse:  
630 immunocytochemical maps, crossed versus uncrossed contributions, and transmitter  
631 colocalization. *J Comp Neurol* 455:406–416.
- 632 Maison SF, Liberman MC (2000) Predicting vulnerability to acoustic injury with a noninvasive  
633 assay of olivocochlear reflex strength. *J Neurosci* 20:4701–4707.
- 634 Maison SF, Luebke AE, Liberman MC, Zuo J (2002) Efferent protection from acoustic injury is  
635 mediated via alpha9 nicotinic acetylcholine receptors on outer hair cells. *J Neurosci*  
636 22:10838–10846.
- 637 Maison SF, Usubuchi H, Liberman MC (2013) Efferent feedback minimizes cochlear neuropathy  
638 from moderate noise exposure. *J Neurosci* 33:5542–5552.
- 639 Matsubara a, Laake JH, Davanger S, Usami S, Ottersen OP (1996) Organization of AMPA  
640 receptor subunits at a glutamate synapse: a quantitative immunogold analysis of hair cell  
641 synapses in the rat organ of Corti. *J Neurosci* 16:4457–4467.
- 642 Meyer AC, Frank T, Khimich D, Hoch G, Riedel D, Chapochnikov NM, Yarin YM, Harke B, Hell

- 643 SW, Egner A, Moser T (2009) Tuning of synapse number, structure and function in the  
644 cochlea. *Nat Neurosci* 12:444–453.
- 645 Murthy V, Taranda J, Elgoyhen AB, Vetter DE (2009) Activity of nAChRs containing alpha9  
646 subunits modulates synapse stabilization via bidirectional signaling programs. *Dev*  
647 *Neurobiol* 69:931–949.
- 648 Ohlemiller KK, Wright JS, Heidbreder AF (2000) Vulnerability to noise-induced hearing loss in  
649 ‘middle-aged’ and young adult mice: a dose–response approach in CBA, C57BL, and  
650 BALB inbred strains. *Hear Res* 149:239–247.
- 651 Omata T, Omata E, Wilhelms HJ, Schätzle W (1992) Neural and infranuclear region changes in  
652 outer hair cells in acoustically exposed rabbits. *Eur Arch Otorhinolaryngol* 249:287–292.
- 653 Pohlert T (2014) The Pairwise Multiple Comparison of Mean Ranks Package (PMCMR). R  
654 Packag:27.
- 655 Pujol R, Puel JL (1999) Excitotoxicity, synaptic repair, and functional recovery in the mammalian  
656 cochlea: a review of recent findings. *Ann N Y Acad Sci* 884:249–254.
- 657 Pujol R, Puel JL, Gervais d’Aldin C, Eybalin M (1993) Pathophysiology of the glutamatergic  
658 synapses in the cochlea. *Acta Otolaryngol* 113:330–334.
- 659 Reiter ER, Liberman MC (1995) Efferent-mediated protection from acoustic overexposure:  
660 relation to slow effects of olivocochlear stimulation. *J Neurophysiol* 73:506–514.
- 661 Ruel J, Wang J, Rebillard G, Eybalin M, Lloyd R, Pujol R, Puel J-L (2007) Physiology,  
662 pharmacology and plasticity at the inner hair cell synaptic complex. *Hear Res* 227:19–27.
- 663 Schaette R, McAlpine D (2011) Tinnitus with a Normal Audiogram: Physiological Evidence for  
664 Hidden Hearing Loss and Computational Model. *J Neurosci* 31:13452–13457.
- 665 Schindelin J, Arganda-Carreras I, Frise E, Kaynig V, Longair M, Pietzsch T, Preibisch S,  
666 Rueden C, Saalfeld S, Schmid B, Tinevez J-Y, White DJ, Hartenstein V, Eliceiri K,  
667 Tomancak P, Cardona A (2012) Fiji: an open-source platform for biological-image analysis.  
668 *Nat Methods* 9:676–682.

- 669 Sergeyenko Y, Lall K, Liberman MC, Kujawa SG (2013) Age-related cochlear synaptopathy: an  
670 early-onset contributor to auditory functional decline. *J Neurosci* 33:13686–13694.
- 671 Shera CA, Guinan JJ (1999) Evoked otoacoustic emissions arise by two fundamentally different  
672 mechanisms: a taxonomy for mammalian OAEs. *J Acoust Soc Am* 105:782–798.
- 673 Simmons DD (2002) Development of the inner ear efferent system across vertebrate species. *J*  
674 *Neurobiol* 53:228–250.
- 675 Simmons DD, Mansdorf NB, Kim JH (1996) Olivocochlear innervation of inner and outer hair  
676 cells during postnatal maturation: Evidence for a waiting period. *J Comp Neurol* 370:551–  
677 562.
- 678 Song Q, Shen P, Li X, Shi L, Liu L, Wang J, Yu Z, Stephen K, Aiken S, Yin S, Wang J (2016)  
679 Coding deficits in hidden hearing loss induced by noise: the nature and impacts. *Sci Rep*  
680 6:25200.
- 681 Suzuki J, Corfas G, Liberman MC (2016) Round-window delivery of neurotrophin 3 regenerates  
682 cochlear synapses after acoustic overexposure. *Sci Rep* 6:24907.
- 683 Taranda J, Maison S, Ballestero J, Katz E, Savino J, Vetter DE, Boulter J, Liberman MC, Fuchs  
684 PA, Elgoyhen AB (2009) A point mutation in the hair cell nicotinic cholinergic receptor  
685 prolongs cochlear inhibition and enhances noise protection. *PLoS Biol* 7:e18.
- 686 Valero MD, Burton JA, Hauser SN, Hackett TA, Ramachandran R, Liberman MC (2017) Noise-  
687 induced cochlear synaptopathy in rhesus monkeys ( *Macaca mulatta* ). *Hear Res*.
- 688 Vetter DE, Liberman MC, Mann J, Barhanin J, Boulter J, Brown MC, Saffiote-Kolman J,  
689 Heinemann SF, Elgoyhen AB (1999) Role of  $\alpha 9$  nicotinic ACh receptor subunits in the  
690 development and function of cochlear efferent innervation. *Neuron* 23:93–103.
- 691 Viana LM, O'Malley JT, Burgess BJ, Jones DD, Oliveira CACP, Santos F, Merchant SN,  
692 Liberman LD, Liberman MC (2015) Cochlear neuropathy in human presbycusis: Confocal  
693 analysis of hidden hearing loss in post-mortem tissue. *Hear Res* 327:78–88.
- 694 Wan G, Gómez-Casati ME, Gigliello AR, Liberman MC, Corfas G (2014) Neurotrophin-3

695 regulates ribbon synapse density in the cochlea and induces synapse regeneration after  
696 acoustic trauma. *Elife* 3:e03564.

697 Wedemeyer C, Vattino LG, Moglie MJ, Ballestero J, Maison SF, Di Guilmi MN, Taranda J,  
698 Liberman MC, Fuchs PA, Katz E, Elgoyhen AB (2018) A Gain-of-Function Mutation in the  
699  $\alpha 9$  Nicotinic Acetylcholine Receptor Alters Medial Olivocochlear Efferent Short Term  
700 Synaptic Plasticity. *J Neurosci*:2528–17.

701 Wedemeyer C, Zorrilla de San Martín J, Ballestero J, Gómez-Casati ME, Torbidoni AV, Fuchs P  
702 a, Bettler B, Elgoyhen AB, Katz E (2013) Activation of presynaptic GABA(B(1a,2))  
703 receptors inhibits synaptic transmission at mammalian inhibitory cholinergic olivocochlear-  
704 hair cell synapses. *J Neurosci* 33:15477–15487.

705 Wiederhold ML, Kiang NY (1970) Effects of electric stimulation of the crossed olivocochlear  
706 bundle on single auditory-nerve fibers in the cat. *J Acoust Soc Am* 48:950–965.

707 Winslow RL, Sachs MB (1988) Single-tone intensity discrimination based on auditory-nerve rate  
708 responses in backgrounds of quiet, noise, and with stimulation of the crossed olivocochlear  
709 bundle. *Hear Res* 35:165–189.

710 Yang L, Chen D, Qu T, Ding T, Yan A, Gong P, Liu Y, Zhang J, Gong S, Yang S, Peng H, Liu K  
711 (2018) Maximal number of pre-synaptic ribbons are formed in cochlear region  
712 corresponding to middle frequency in mice. *Acta Otolaryngol* 138:25–30.

713 Young ED, Barta PE (1986) Rate responses of auditory nerve fibers to tones in noise near  
714 masked threshold. *J Acoust Soc Am* 79:426–442.

715 Zachary SP, Fuchs PA (2015) Re-Emergent Inhibition of Cochlear Inner Hair Cells in a Mouse  
716 Model of Hearing Loss. *J Neurosci* 35:9701–9706.

717

718



719 **Figure Legends**720 **Figure 1: Auditory function in unexposed WT, *Chrna9* KO and *Chrna9L9'T* KI mice.**

721 (a) ABRs thresholds for control WT (n=12), *Chrna9* KO (n=14) and *Chrna9L9'T* KI (n=15) mice  
722 at P21. (b) ABR peak 1 amplitudes at 80 dB SPL. (c) DPOAEs thresholds in the same  
723 unexposed mice in the different genotypes. Cochlear thresholds are elevated in *Chrna9L9'T* KI  
724 ears, as measured by either ABRs (a) or DPOAEs (c). In all cases median and interquartile  
725 ranges are shown and the comparisons were made by a Kruskal-Wallis non-parametric ANOVA  
726 followed by a Dunn's post-test. Dark grey asterisks represent the statistical significance  
727 between *Chrna9* KO and WT and light gray asterisks between *Chrna9L9'T* KI and WT mice  
728 (\*= $p<0.05$  and \*\*= $p<0.01$ ).

729

730 **Figure 2. ABR measurements before and after acoustic trauma (AT).**

731 (a) Representative ABRs traces from WT, *Chrna9* KO and *Chrna9L9'T* KI mice at P21 before  
732 trauma (Pre-AT, black trace), 1 day after AT (AT+1d, dark gray trace) and 7 days after AT  
733 (AT+7d, light gray trace). Arrow indicates peak 1 amplitude. Scale bars: vertical=0.4  $\mu$ V,  
734 horizontal=1 ms (b) ABR thresholds in WT (n=12), *Chrna9* KO (n=14) and *Chrna9L9'T* KI (n=15)  
735 mice at P21 before trauma, 1 day after AT and 7 days after AT. WT and *Chrna9* KO mice  
736 showed a significant increase in ABR thresholds 1 day after AT. A recovery of ABR thresholds  
737 was observed a week after exposure only in WT mice. *Chrna9L9'T* KI mice did not present any  
738 changes in ABR thresholds at any time after AT. (c) ABR peak 1 amplitudes at 80 dB SPL in  
739 WT, *Chrna9* KO and *Chrna9L9'T* KI mice at the same time points shown in (b). WT and *Chrna9*  
740 KO mice displayed a reduction in amplitudes 1 day after AT and only a partial recovery a week  
741 after exposure. Peak 1 amplitudes in *Chrna9L9'T* KI mice were unaffected by noise exposure.  
742 (d) ABR peak 1 latencies in WT, *Chrna9* KO and *Chrna9L9'T* KI mice at the same time points  
743 shown in (b). Latencies were not affected in any of the genotypes after AT. Median and  
744 interquartile ranges are shown and the comparisons were made by Friedman tests followed by

745 a post-hoc test. Dark grey asterisks represent the statistical significance of AT+1d values  
746 compared to Pre-AT and light gray asterisks represent AT+7d values compared to Pre-AT  
747 controls. (\*= $p<0.05$ ; \*\*= $p<0.01$ ; \*\*\*= $p<0.001$ ).

748

749 **Figure 3. Analysis of IHCs ribbon synapses in unexposed WT, *Chrna9* KO and**  
750 ***Chrna9L9'T* KI mice.**

751 Quantitative data obtained from unexposed WT, *Chrna9* KO and *Chrna9L9'T* KI mice at P28.  
752 For each IHC we analyzed the number of CtBP2 puncta, post-synaptic GluA2 receptor patches,  
753 and putative ribbon synapses, defined as juxtaposed CtBP2 and GluA2 positive puncta.  
754 Horizontal lines inside the boxplots represent the median and whiskers correspond to  
755 percentiles 10 to 90. Comparisons were made by a Kruskal-Wallis non-parametric ANOVA  
756 followed by a Dunn's post-test. Dark grey asterisks represent the statistical significance  
757 between *Chrna9* KO and WT and light gray asterisks between *Chrna9L9'T* KI and WT mice  
758 (\*= $p<0.05$ ; \*\*= $p<0.01$ ; \*\*\*= $p<0.001$ ).

759

760 **Figure 4. Analysis of the degree of IHC synaptopathy a week after AT.**

761 **Left panel:** representative confocal images of IHCs synapses from cochleae immunolabeled for  
762 pre-synaptic ribbons (CtBP2-red) and post-synaptic receptor patches (GluA2-green) (scale  
763 bar=10  $\mu\text{m}$ ). The dashed lines show the approximate outline of one IHC. CtBP2 antibody also  
764 weakly stains IHC nuclei. **Right panel:** Quantitative data obtained from WT, *Chrna9* KO and  
765 *Chrna9L9'T* KI mice at P28. For each IHC we analyzed the number of CtBP2 puncta, post-  
766 synaptic GluA2 receptor patches, and putative ribbon synapses. (a) In traumatized WT mice  
767 there was a reduction in the number of CtBP2 puncta, GluA2 receptor patches and putative  
768 synapse, depending on cochlear frequency/location ( $n_{\text{WT}_{\text{control}}}=360$  IHCs at the apical, 350  
769 IHCs at the medial and 185 IHCs at the basal region from 8-10 animals;  $n_{\text{WT}_{\text{AT+7d}}}=394$  IHCs at

770 the apical, 492 IHCs at the medial and 166 IHCs at the basal region from 6-11 animals). (b) In  
771 traumatized *Chrna9* KO mice there was a reduction in the number of pre, post and colocalized  
772 puncta that was more pronounced at the basal turn ( $n_{KO_{control}}=234$  IHCs at the apical, 200 IHCs  
773 at the medial and 218 IHCs at the basal region from 6-8 animals;  $n_{KO_{AT+7d}}=291$  IHCs at the  
774 apical, 271 IHCs at the medial and 130 IHCs at the basal region from 4-7 animals). (c) In  
775 traumatized *Chrna9L9'T* KI mice we found a significant increase in the number of pre-synaptic  
776 ribbons, postsynaptic AMPA receptors and colocalization puncta for the three regions of the  
777 cochlea ( $n_{KI_{control}}=262$  IHCs at the apical, 309 IHCs at the medial and 135 IHCs at the basal  
778 region from 7-12 animals;  $n_{KI_{AT+7d}}=179$  IHCs at the apical, 406 IHCs at the medial and 119  
779 IHCs at the basal region from 5-14 animals). Horizontal lines inside the boxplots represent the  
780 median and whiskers correspond to percentiles 10 to 90. Comparisons were made by a  
781 Kruskal-Wallis non-parametric ANOVA followed by a Dunn's post-test (\*= $p<0.05$ ; \*\*= $p<0.01$ ;  
782 \*\*\*= $p<0.001$ ).

783

784 **Figure 5. Evaluation of OHCs functional integrity before and after AT.**

785 DPOAEs thresholds for WT ( $n=12$ ), *Chrna9* KO ( $n=13$ ) and *Chrna9L9'T* KI ( $n=11$ ) mice at the  
786 same time points as in Figure 2. DPOAEs thresholds showed a significant increase 1 day after  
787 AT in WT and *Chrna9* KO, but not in *Chrna9L9'T* KI mice. 7 days after AT, DPOAEs thresholds  
788 recovered only in WT whereas DPOAEs thresholds remain elevated in *Chrna9* KO mice.  
789 Median and interquartile ranges are shown and the comparisons were made by Friedman tests  
790 followed by a post-hoc test. Dark grey asterisks represent the statistical significance of AT+1d  
791 values compared to Pre-AT and light gray asterisks represent AT+7d values compared to Pre-  
792 AT controls. (\*= $p<0.05$ ; \*\*= $p<0.01$ ; \*\*\*= $p<0.001$ ).

793

794 **Figure 6. Olivocochlear synaptic boutons a week after AT.**

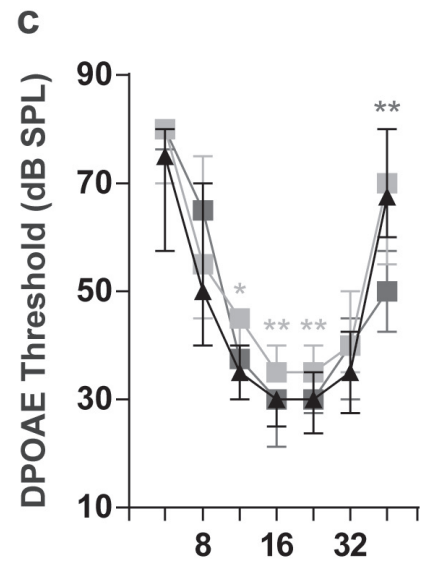
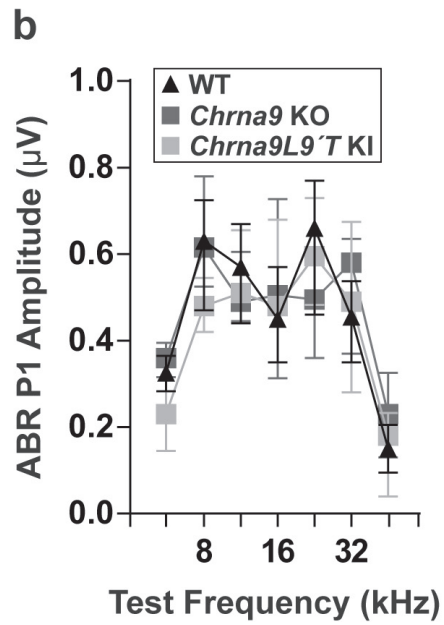
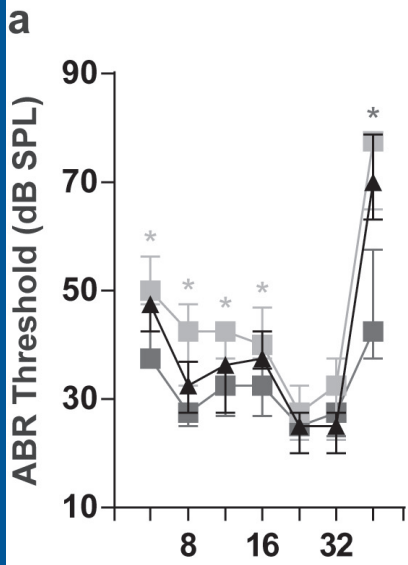
795 (a) Synaptophysin immunostaining of the OHC region in control and traumatized WT, *Chrna9*  
796 KO and *Chrna9L9'T* KI mice at P28 reveals MOC terminals under OHCs (scale bar=10  $\mu$ m). In  
797 WT ears, MOC terminals regularly occurred as clusters, such as the quadruplet indicated by  
798 four arrows. After AT, there was a reduction in the number of MOC terminals per OHC. In  
799 *Chrna9* KO, most terminals occurred as singlet or doublet indicated by one or two arrows,  
800 respectively. After AT, there was no alteration in the number of efferent contacts. In *Chrna9L9'T*  
801 KI mice, each OHC is contacted by a larger than normal contingent of MOC terminals (arrows)  
802 with no modification after AT. (b) Cumulative frequency histograms of the efferent innervation  
803 pattern to OHCs in control and 7 days after AT in the different genotypes ( $n_{WT_{control}}=1418$  OHCs  
804 from 8 animals,  $n_{WT_{AT+7d}}=2226$  OHCs from 6 animals,  $n_{KO_{control}}=2017$  OHCs from 8 animals,  
805  $n_{KO_{AT+7d}}=1319$  from 7 animals,  $n_{KI_{control}}=2860$  OHCs from 10 animals and  $n_{KI_{AT+7d}}=1795$  OHCs  
806 from 8 animals). (c) Synaptophysin immunostaining of the inner spiral bundle (ISB) region in  
807 control and traumatized WT, *Chrna9* KO and *Chrna9L9'T* KI mice (scale bar=10  $\mu$ m). The  
808 dashed lines show the approximate outline of one IHC. WT mice exhibit a regular progression of  
809 efferent terminals along the modiolar side of the IHCs (ISB; arrows). These boutons are larger  
810 than those on the pillar side of the IHC (arrowheads). After AT, there was no alteration in the  
811 efferent innervation pattern. In *Chrna9* KO, there was a reduction in efferent synapses on the  
812 pillar side that was not modified after AT. In *Chrna9L9'T* KI mice, there was an increase of  
813 efferent terminals on the pillar side with no modification after AT.

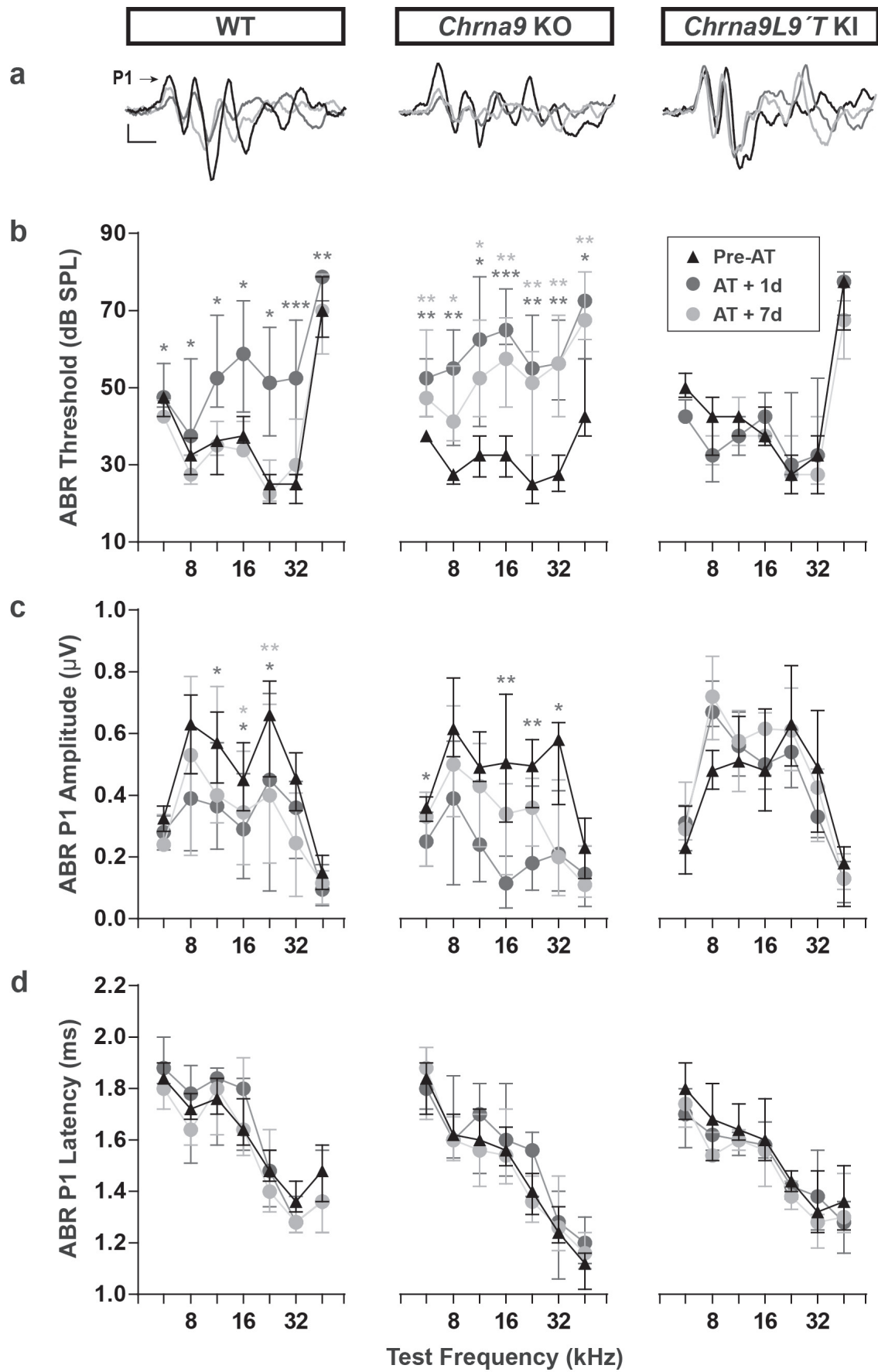
814

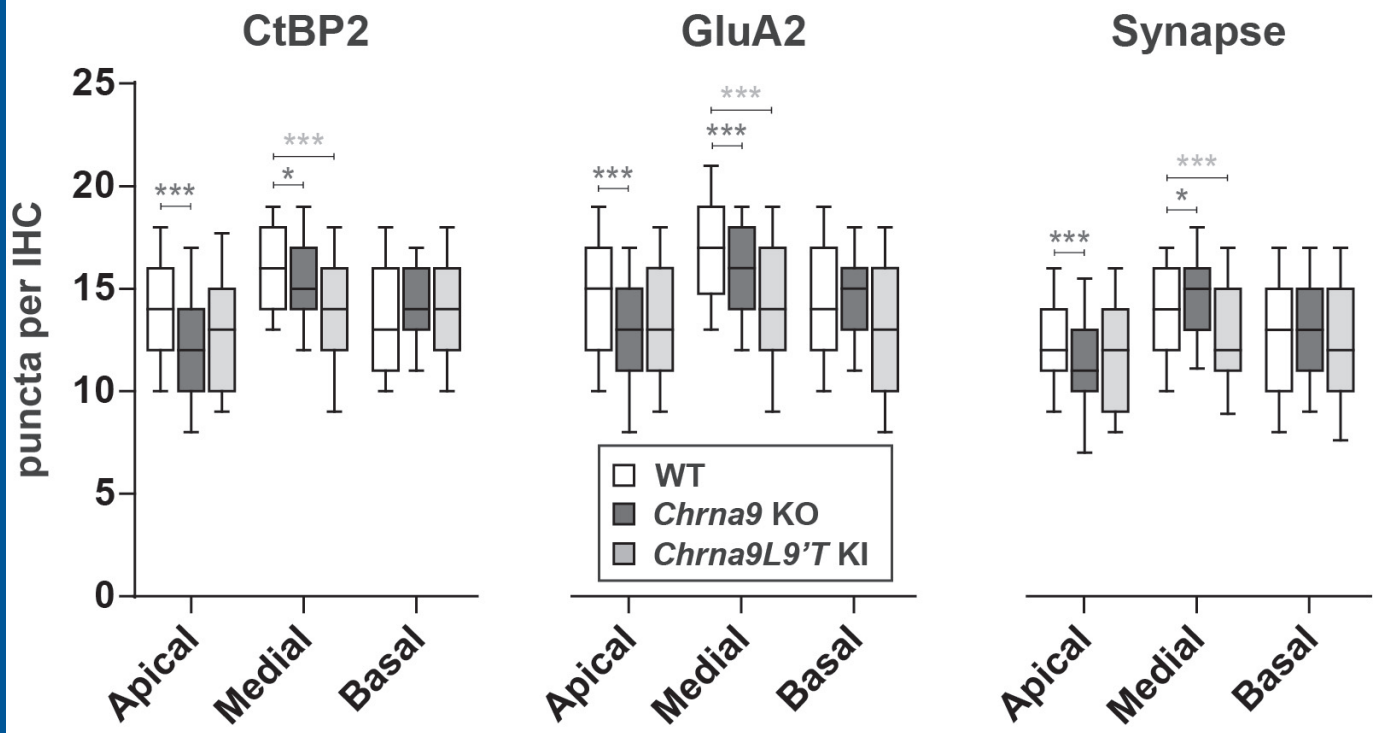
815 **Figure 7. Auditory function and OHC connectivity after a second noise exposure in WT**  
816 **mice.**

817 7 days after AT, WT mice were traumatized again with the same acoustic protocol (n=6 animals).  
818 (a) ABR thresholds of WT control, 1 day after AT (AT+1d), 7 days after AT (AT+7d), 1 day after  
819 a second noise exposure (2AT+1d) and 7 days after the second trauma (2AT+7d). There were  
820 large threshold elevations both the day after the first and the second AT with a complete

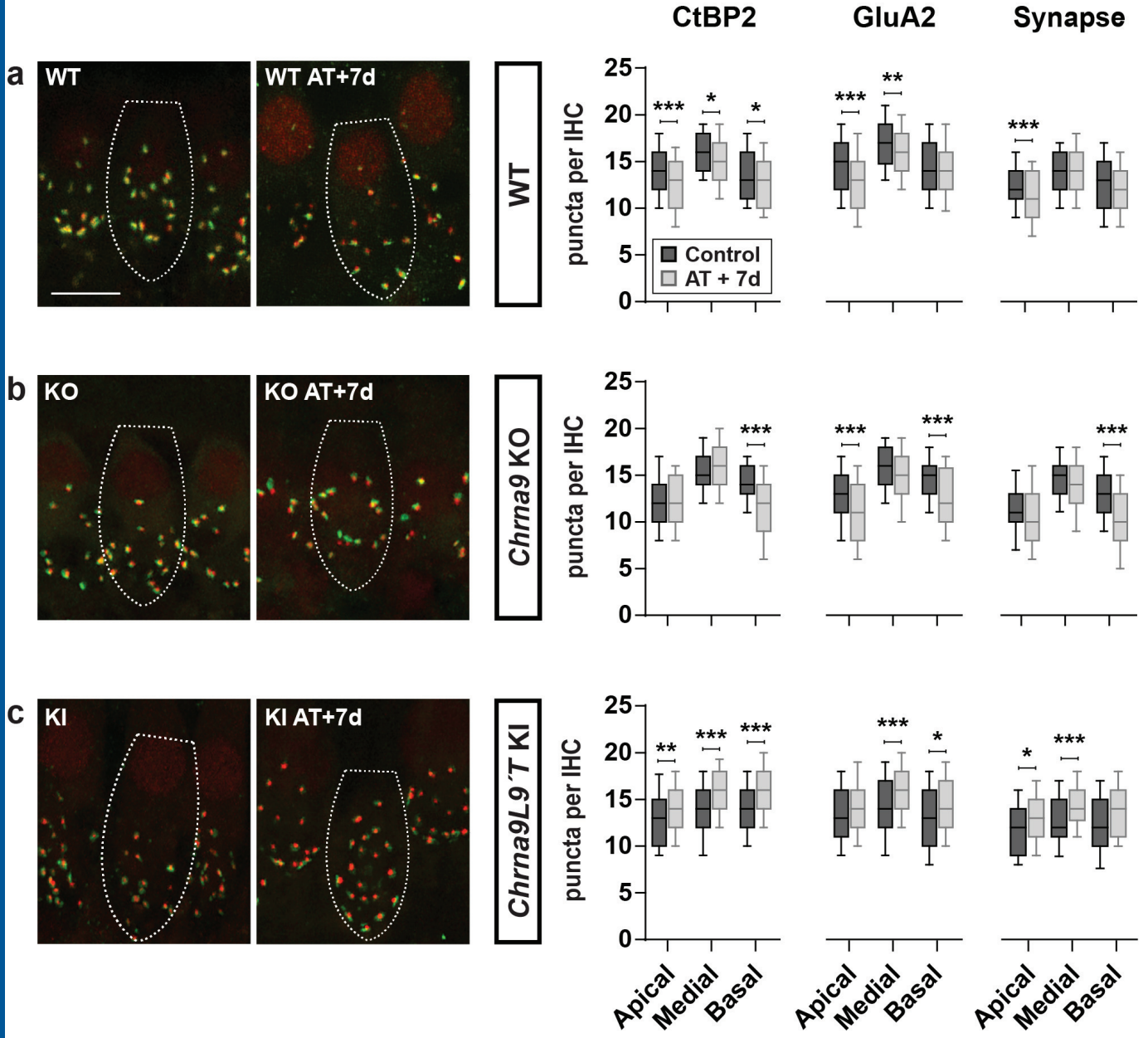
821 recovery 7 days after either acoustic overexposure. Median and interquartile ranges are shown  
822 and the comparisons were made by Friedman tests followed by a post-hoc test. Grey asterisks  
823 represent the statistical significance of AT+7d values compared to 2AT+1d (\*= $p<0.05$ ;  
824 \*\*= $p<0.01$ ). **(b)** Cumulative frequency histograms of MOC innervation pattern after the first and  
825 the second noise exposure. Data corresponding to P21 control mice (Control P21) and 7 days  
826 after AT (AT+7d) are the same as shown in Figure 6. After the second noise exposure, there  
827 was not any further reduction in the number of MOC synapses to OHC. We also showed the  
828 quantification of MOC terminals in unexposed P35 control mice and found no difference  
829 compared to unexposed P28 mice.

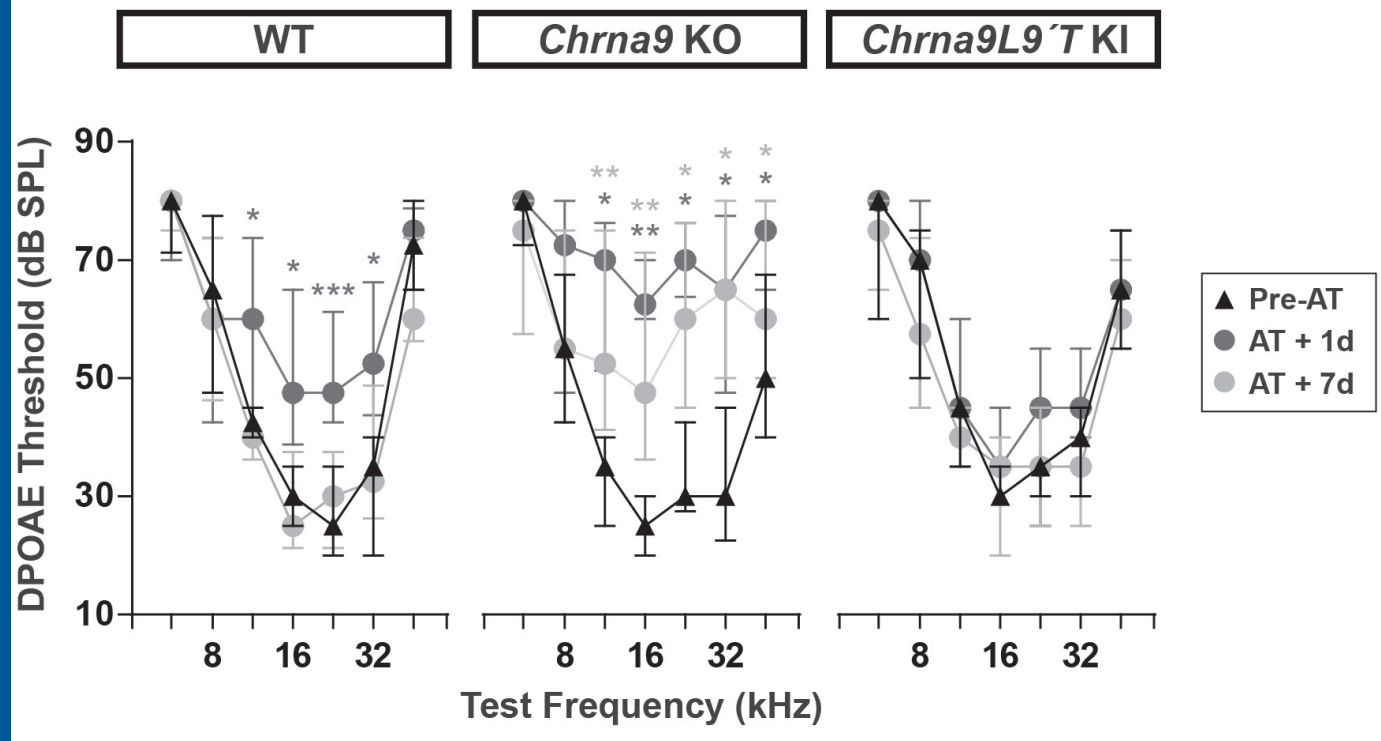


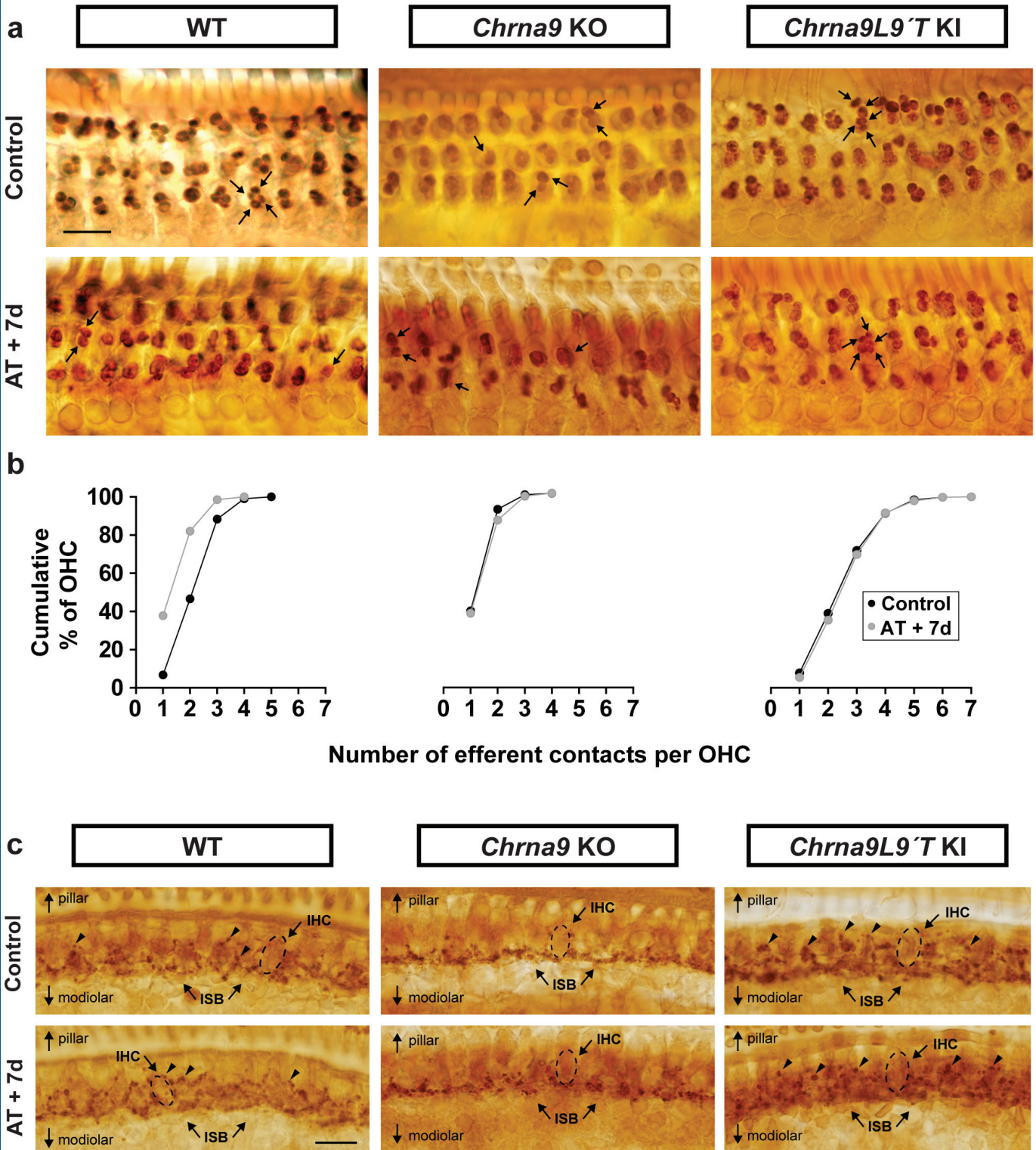




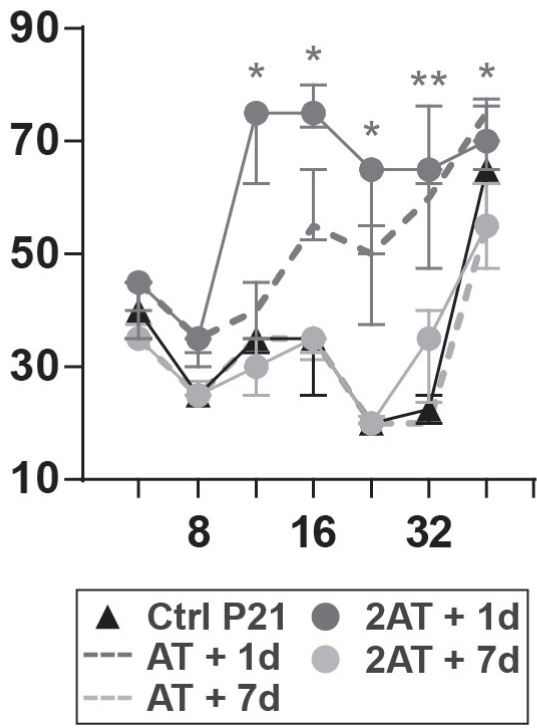








**a**  
ABR Threshold (dB SPL)



**b**

